Research Journal of Applied Sciences 6 (1): 53-60, 2011
ISSN: 1815-932X

The Effects of Nonlinear Gain and Thermal Carrier Escape on Dynamic Characterizations of GaAs/InGaAs Self-Assembled Quantum Dot Lasers

H. Arabshahi and D. Ghodsi Nahri
Department of Physics, Mashhad Branch, Islamic Azad University, Mashhad, Iran

Abstract: In this study researchers have studied the effects of nonlinear gain and thermal carrier escape on dynamic characteristics of GaAs/InGaAs self-assembled quantum dot laser with considering the homogeneous and inhomogeneous broadening of the optical gain using fourth order Runge-Kutta method. The calculations show that the thermal carrier escape leads to shift the dominant lasing mode at the low injection currents. The number of lasing modes increases for the larger injection currents. With exceeding the FWHM of homogeneous broadening from the full width at half maximum FWHM of inhomogeneous broadening, the dynamic and static characteristics degrade and SAQD-LD reaches the steady-state slower. The threshold current, the steady-state photons and the dynamic-characteristics degrade and SAQD-LD reaches the steady-state slower as the FWHM of inhomogeneous broadening and carrier relaxation life time increase.

Key words: Nonlinear gain, self-assembled quantum dot laser, Runge-Kutta method, thermal carrier escape, homegeneous, inhomogeneous

INTRODUCTION

Three-dimensional quantum confinement of electrons, holes and excitons in semiconductor microstructures known as quantum dots is predicted to produce new physical phenomena and improve optoelectronic devices significantly (Zhang *et al*., 2008; Liu *et al*., 2005; Lv *et al*., 2008). The atom like state density in quantum dots associated with three dimensional confinement of electrons and holes would cause an increase of optical gain and limit thermal carrier distribution.

Therefore, the use of quantum dots for semiconductor lasers as an active region is expected to provide a remarkable reduction of threshold current and temperature sensitivity. During primary research based on predictions in the early 1980s, quantum dots have been created by combining lithography and re-growth on a processed substrate.

The artificial techniques however, suffer from non-uniform doe size, poor interface quality and low numerical density. High uniformity is required to achieve the atom-like state density of a dot ensemble. A high optical quality and high numerical density are required to obtain a large gain. Quantum dot lasers using artificial techniques therefore, showed a high threshold current density (Sugawara, 1999; Sugawara *et al*., 2000). In this study, considering the homogeneous and inhomogeneous broadening of the optical gain also without and with considering the nonlinear gain and thermal escape of carriers from QDs, researchers solve the rate equations numerically using fourth-order Runge-Kutta method and analyze the dynamics characteristics of GaAs/InGaAs SAQD-LDs.

We show that considering the nonlinear gain result in the dynamic-characteristic of photons number at the FWHM of homogeneous broadening comparable, near or equal to the FWHM of inhomogeneous broadening reaches the steady-state faster.

The dynamics characteristics such as maximum of the relaxation oscillation magnitude, turn-on delay, relaxation oscillation frequency and modulation bandwidth also the steady-state photons number improve as the current increases. Threshold current, turn-on delay and steady-state photons number increase and relaxation oscillation frequency decreases for larger FWHM of homogeneous broadening.

LINEAR AND NONLINEAR OPTICAL GAIN

Based on the density-matrix theory, the linear optical gain of QD active region is given as Bilenca and Eisenstein (2004):

$$g^{(1)}(E)=\frac{2pe^2hN_D}{cn_re_0m_0^2}\times\frac{\left|p_{cv}^s\right|(f_c-f_v)}{E_{cv}}B_{cv}(E-E_{cv}) \quad (1)$$

Corresponding Author: H. Arabshahi, Department of Physics, Mashhad Branch, Islamic Azad University, Mashhad, Iran

Where:

n_r = The refractive index
N_D = The volume density of QDs
$|P^{\sigma}_{cv}|^2$ = The transition matrix element
f_c = The electron occupation function of the conduction-band discrete state
f_v = That of the valence-band discrete state
E_{cv} = The interband transition energy

The linear optical gain shows the homogeneous broadening of a Lorentz shape as Bilenca and Eisenstein (2004):

$$B_{cv}(E-E_{cv})=\frac{hG_{cv}/p}{(E-E_{cv})^2+(hG_{cv})^2} \quad (2)$$

Where FWHM is given as $2h\Gamma_{cv}$ with polarization dephasing or scattering rate Γ_{cv}. Neglecting the optical-field polarization dependence, the transition matrix element is given as:

$$\left|P^{s}_{cv}\right|^2=\left|I_{cv}\right|^2 M^2 \quad (3)$$

where, I_{cv} represents the overlap integral between the envelope functions of an electron and a hole:

$$M^2=\frac{m_0^2}{12m_e^*}\times\frac{E_g(E_g+D)}{E_g+2D/3} \quad (4)$$

Where:

k.p = The interaction between the conduction band and valence band
E_g = The band gap
m_e* = The electron effective mass
E_g = The spin-orbit interaction energy of the QD material

Equation 3 holds as long as we consider QDs with a nearly symmetrical shape (Tan *et al*., 2007, 2008). In actual SAQD-LDs, we should rewrite the linear optical gain formula of Eq. 1 by taking into account inhomogeneous broadening due to the QD size and composition fluctuation in terms of a convolution integral as:

$$g^{(1)}(E)=\frac{2pe^2hN_D}{cn_re_0^2}.\frac{\left|p^{s}_{cv}\right|^2}{E_{cv}}(f_c(E)-f_v(E)).$$
$$B_{cv}(E-E_c)G(E_c-E_{cv})dE_c \quad (5)$$

Where:

E_{cv} = The center of the energy distribution function of each interband transition
$f_c(E_c)$ = The electron occupation function of the conduction-band discrete state of the QDs with the interband transition energy of E_c
$f_v(E_v)$ = That of the valence band discrete state

The energy fluctuation of QDs are represented by G (E_c-E_{cv}) that takes a Gaussian distribution function as:

$$G(E_c-E_{cv})=\frac{1}{\sqrt{2p}x_0}\exp(E_c-E_{cv})^2/2x_0^2 \quad (6)$$

Whose FWHM is given by $\Gamma_0 = 2.35\xi_0$. The width Γ_0 usually depends on the band index c and v (Sugawara *et al*., 2000).

RATE EQUATIONS

The most popular and useful way to deal with carrier and photon dynamics in lasers is to solve rate equations for carrier and photons (Markus *et al*., 2003; Grundmann, 2002). Researchers consider an electron and a hole as an exciton, thus, the relaxation means the process that both an electron and a hole relax into the ground state simultaneously to form an exciton. We assume that only a single discrete electron and hole ground state is formed inside the QD and the charge neutrality always holds in each QD.

In order to describe the interaction between the QDs with different resonant energies through photons, we divide the QD ensemble into j = 1, 2,... 2M+1 groups, depending on their resonant energy for the interband transition over the longitudinal cavity photon modes. j = m corresponds to the group and mode at E_{cv}. We take the energy width of each group equal to the mode separation of the longitudinal cavity photon modes which equals to:

$$D_E=ch/2n_rL_{ca} \quad (7)$$

where, L_{ca} is the cavity length. The energy of the jth QDs group is represented by:

$$E_j=E_{cv}-(M-j)D_E \quad (8)$$

Where j = 1, 2,....,2M+1. The QD density jth QDs group is given as:

$$N_DG_j=N_DG(E_j-E_{cv})D_E \quad (9)$$

Let N_j be the carrier number in jth QDs group according to Pauli's exclusion principle, the occupation probability in the ground state of the jth QDs group is defined as:

$$P_j = N_j / 2N_D V_a G_j \quad (10)$$

The rate equations are as follows (Tan *et al*., 2008)

$$\frac{dN_s}{dt} = \frac{I}{e} - \frac{N_s}{\tau_s} - \frac{N_s}{\tau_{sr}} + \frac{N_w}{\tau_{we}} \quad (11)$$

$$\frac{dN_w}{dt} = \frac{N_s}{\tau_s} + \frac{N_j}{\tau_e D_g} - \frac{N_w}{\tau_{wr}} - \frac{N_w}{\tau_{we}} - \frac{N_w}{\tau_d}$$

$$\frac{dNj}{dt} = \frac{N_w G_j}{\tau_{dj}} - \frac{N_j}{\tau_r} - \frac{N_j}{\tau_e D_j} - \frac{c\Gamma}{n_r}.g^{(l)}(E)S_m$$

$$\frac{dSm}{dt} = \frac{\beta N_j}{\tau_r} + \frac{c\Gamma}{n_r}.g^{(l)}(E)S_m - S_m/\tau_p$$

where, N_S, N_w and N_j are the carrier number in Separate Confinement Heterostructure (SCH) layer, Wetting Layer (WL) and jth QDs group, respectively, S_m is the photon number of mth mode where m = 1,2...2M+1, I is the injected current, G_j is the fraction of the jth QDs group type within an ensemble of different dot size populations, e is the electron charge, D_g is the degeneracy of the QD ground state without spin, β is the spontaneous-emission coupling efficiency to the lasing mode. $g_{mj}^{(1)}$ is the linear optical gain which the jth QDs group gives to the mth mode photons where is represented by:

$$g_{mj}^{(l)}(E) = \frac{2\pi e^2 h N_D}{c n_r \varepsilon_0 e_0^2}.\frac{|p_{cv}^s|^2}{E_{cv}}(2p_j - 1).\ G_j B_{cv}(E_m - E_j) \quad (12)$$

The related time constants are as τ_s, diffusion in the SCH region, τ_{sr}, carrier recombination in the SCH region, τ_{we}, carrier reexcitation from the WL to the SCH region, τ_{wr}, carrier recombination in the WL, τ_{dj}, carrier relaxation into the jth QDs group, τ_r, carrier recombination in the QDs, τ_p, photon lifetime in the cavity, The average carrier relaxation lifetime, $\bar{\tau}_d$ is given as:

$$\tau_d^{-1} = \tau_{dh}^{-1}.G_n = \tau_d^{-1}(1 - P_n)G_n \quad (13)$$

where, τ_0 is the initial carrier relaxation lifetime. The photon lifetime in the cavity is:

$$\tau_p^{-1} = c/n_r + \ln(1/R_1R_2)/2L_{cav} \quad (14)$$

where, R_1 and R_2 are the cavity mirror reflectivity and α_i is the internal loss. The laser output power of the mth mode from one cavity mirror is given a:

$$I_m = hw_m cS_m \ln(1/R)/2L_{cav}n_r \quad (15)$$

where, w_m is the emitted photon frequency and R is R_1 or R_2. We solved the rate equations numerically using fourth order Runge-Kutta method (Sugawara, 1995) to obtain the carrier and photon characteristics and modulation response by supplying the steplike current at time t = 0.

The system reaches the steady-state after the relaxation oscillation. We assume that all the carriers are injected into the WL, i.e., $\tau_{sr} = \tau_{we} = \infty$ and consider the thermal carrier escape time $\tau_e = \infty$.

ANALYSIS OF THE EFFECTS OF NONLINEAR GAIN AND THERMAL CARRIER ESCAPE ON DYNAMIC CHARACTERISTICS

We simulated previous characteristics with considering the nonlinear gain and thermal carrier escape. The simulation results are similar to previous results except to follow cases. Figure 1 shows photon characteristics for different injection currents I = 2, 2.5, 5 and 10 mA when the FWHM of homogeneous considering the nonlinear gain and thermal carrier escape from QDs.

As shown in Fig. 1a, the lasing photons at I = 5 and 10 mA reach the steady-state after 40 and 30 nsec. It is also seen from Fig. 1b that the lasing photons at I = 5 and 10 mA do not reach lesser than that of I = 2 mA and reach the steady-state after 80 and 70 nsec. Lasing photons at I = 10 mA do not reach lesser than that of I = 5 mA and the lasing photons at I = 2.5 mA reach the steady-state after 60 nsec.

As shown in Fig. 1c, the lasing photons at I = 5 and 10 mA after than 20 and 10 ns and that of I = 2.5 mA after 30 nsec reach the steady-state. Also it is shown in Fig. 1d that the dynamic-characteristics of the Room-Temperature (RT) operation of SAQD-LDs, the lasing photons at I = 5 and 10 mA reach the steady-state after 40 and 30 nsec.

These non steady-states, unlike previous case that we do not consider the nonlinear gain and thermal carrier escape, decreases with increasing the injection current. Figure 2 shows RT photon-characteristics for the central lasing mode and close modes around it at currents I = 2.1, 2.15, 5 and 10 mA.

As shown in Fig. 2a, maximum of the lasing photons are relate to the mode M-1. This shift of dominant lasing mode is due to the thermal carrier escape effect which it wastes with increasing the injection current (Fig. 2c and d). Researchers see that the lasing photons at the small

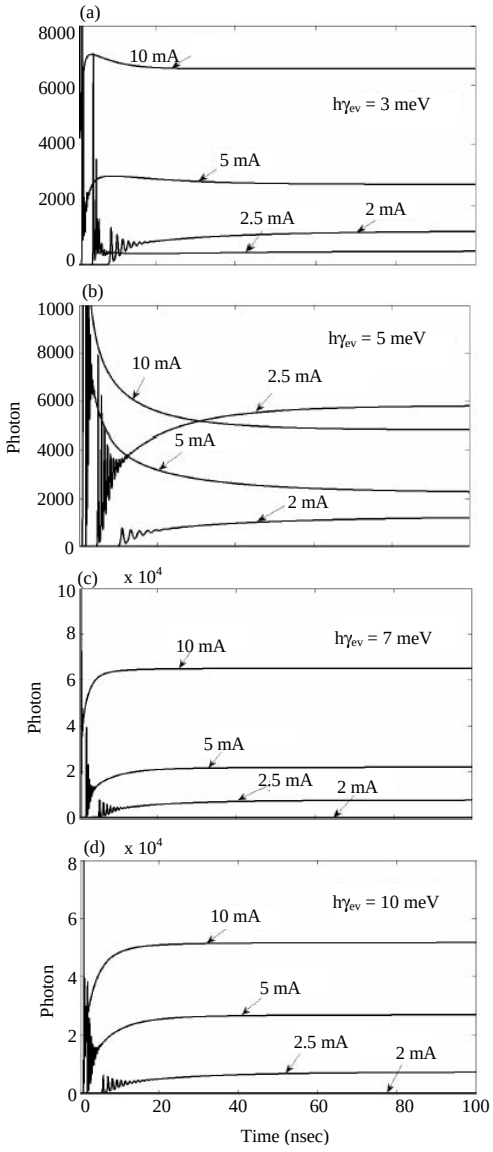

Fig. 1: Photon-characteristics for different injection currents I = 2, 2.5, 5 and 10 mA when the FWHM of homogeneous broadening is (a) 3 meV, (b) 5 meV, (c) 7 meV and (d) 10 meV with considering the nonlinear gain and thermal carrier escape from Qds

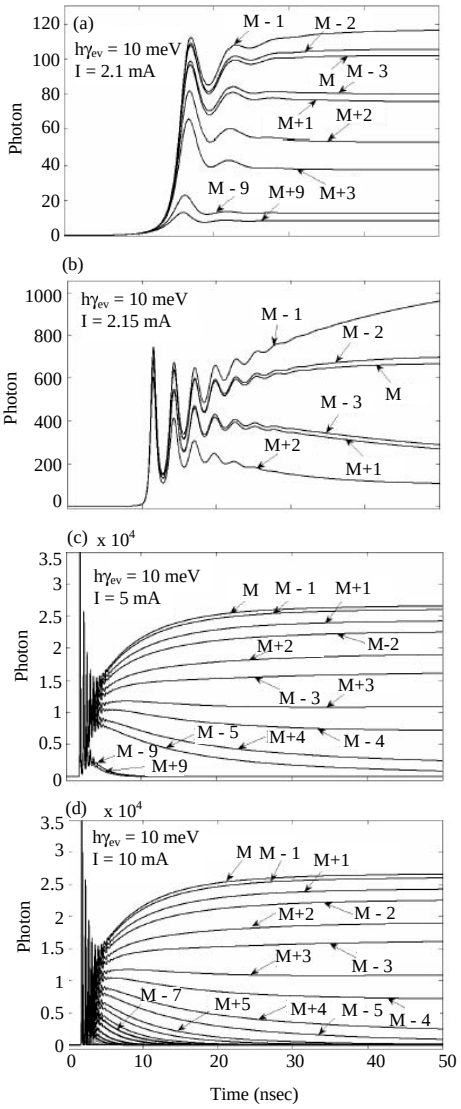

Fig. 2: RT photon-characteristics for the central lasing mode and close modes around it at currents I = 2.1, 2.15, 5 and 10 mA

FWHM of homogeneous broadening that all of the different QD groups having an optical gain larger than threshold gain laze independently or nearly independently, reach the steady-state after finishing the relaxation oscillation but at the FWHM of homogeneous broadening comparable, near or equal to the FWHM of inhomogeneous broadening without considering the nonlinear gain, the central mode photons, at the time of relaxation oscillation and after finishing it, receive gain not only from the central group of QDs but also from more or all the groups infinitely, since carriers of these groups do intra band relaxation and put into the central lasing mode by the stimulated emission as a result, lasing emission with one line occurs (Bilenca and Eisenstein, 2004) and the central mode photons increase infinitely. When we consider the total gain at the FWHM of homogeneous broadening near or equal to the FWHM of inhomogeneous broadening, the central mode photons at the time of relaxation oscillation and after finishing it, increase and after several nanoseconds reach the steady-state. This is because, the carriers of QDs group which lie within the FWHM of inhomogeneous

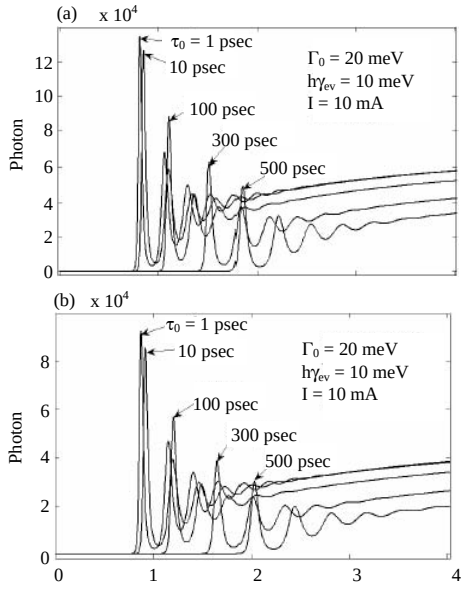

Fig. 3: Simulation results for the RT lasing at different initial carrier relaxation lifetimes 1, 10, 100, 300 and 500 psec at (a) 10 meV and (b) 20 meV

broadening of the central mode, do intra band relaxation and emit into the central lasing mode and close modes around it, the number of these modes and value of emitting into them increase with increasing the injection current. This emission becomes fixing after several nanoseconds due to the gain saturation. As a result, lasing emission with multimode occurs. At the FWHM of homogeneous broadening comparable to the FWHM of inhomogeneous broadening, 3 meV at the injection currents I = 2.5, 5 and 10 mA and 5 meV at the injection currents I = 5 and 10 mA, the central mode photons decrease due to emitting the central group carriers into other modes (Fig. 1a and b).

They becomes fixing after several nanoseconds as result of the gain saturation at those modes. We treat the effects of the carrier relaxation lifetime and inhomogeneous broadening on dynamic characteristics. Figure 3 shows the simulation results of photon characteristics with considering the nonlinear gain and thermal carrier escape, for the RT lasing at different initial carrier relaxation lifetimes of 1, 10, 100, 300 and 500 psec at the FWHM of inhomogeneous broadenings 10 meV and 20 meV. As shown in Fig. 4 with increasing the carrier relaxation lifetime, maximum of the relaxation oscillation magnitude and the steady-state photons decrease, turn-on delay also increases. Turn-on delay increases as the inhomogeneous broadening increases because both of central group and other groups DOS decrease as carriers

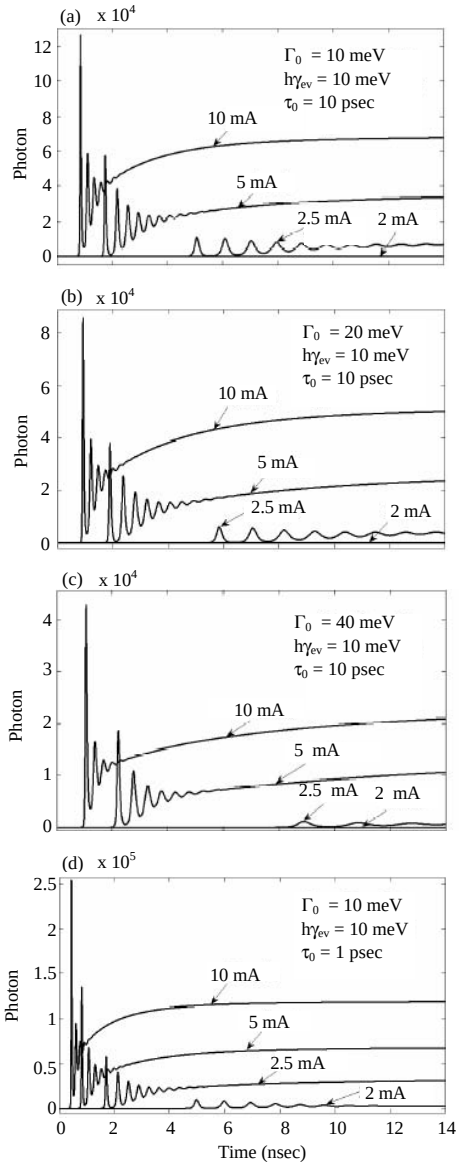

Fig. 4: Calculated results for the FWHM of inhomogeneous broadenings (a) 10 meV, (b) 20 meV and (c) 40 meV at the initial carrier relaxation lifetime 10 psec and (d) 10 meV at the initial carrier relaxation life time 1 psec for different injection currents I = 2, 2.5, 5 and 10 mA

that emit into the central mode decrease more than decreasing the number of states of the central group. Figure 5 shows calculated results for the FWHM of inhomogeneous broadenings (a) 10 meV, (b) 20 meV and (c) 40 meV at the initial carrier relaxation lifetime 10 psec and (d) 10 meV at the initial carrier relaxation lifetime 1 psec for different injection currents I = 2, 2.5, 5 and 10 mA. As shown in Fig. 4 with increasing the inhomogeneous

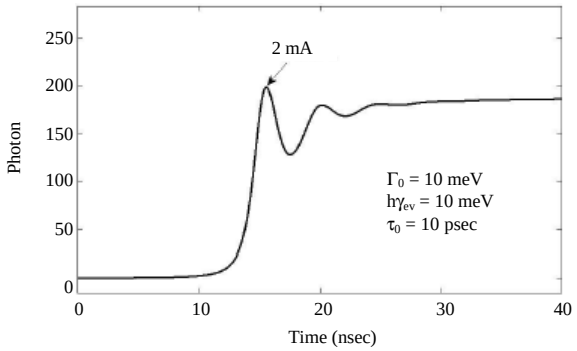

Fig. 5: Lasing photons at the injection current 2 mA for the FWHM of inhomogeneous broadening 10 meV

broadening, the maximum of the relaxation oscillation magnitude and the steady-state photons decrease, laser reaches the steady-state slower. The threshold current also increases because the carriers that emit into the central mode decrease more than decreasing the number of states of the central group. Figure 4 shows the lasing photons at the injection current I = 2 mA for the FWHM of inhomogeneous broadening 10 meV.

As shown in Fig. 5, there is the lasing emission unlike Fig. 3b. Comparing Fig. 3a and 3d, the threshold current increases and the relaxation oscillation frequency decreases, laser also reaches the steady-state slower as the carrier relaxation lifetime increases due to increasing consumption of carriers in WL.

Figure 6 shows the photon-characteristics at the FWHM of homogeneous broadenings (a) 10 meV, (b) 15 meV, (c) 20 meV and (d) 30 meV and injection currents I = 2, 2.5, 5 and 10 mA for the FWHM of inhomogeneous broadening 20 meV.

As shown in Fig. 6 with exceeding the FWHM of homogeneous broadening from the FWHM of inhomogeneous broadening, maximum of the relaxation oscillation magnitude and the steady-state photons decrease, turn-on delay and the threshold current increase. Relaxation oscillation frequency until the FWHM of homogeneous broadening 40 meV decreases and then increases, laser also reaches the steady-state slower.

As a result with exceeding the homogeneous broadening from the inhomogeneous broadening, the dynamic and static-characteristics of SAQD-LD degrade due to increasing the empty DOS. We also simulated the modulation response of GaAs/InGaAs SAQD-LD with considering the nonlinear gain and thermal carrier escape. Figure 7 shows the simulation results for the RT lasing at different injection currents 2.5, 5, 7.5, 12.5.

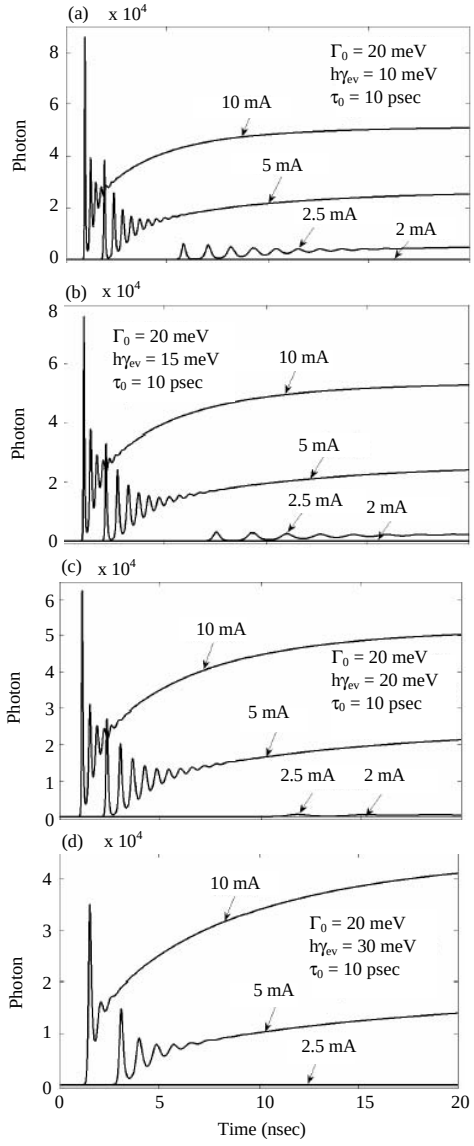

Fig. 6: Photon-characteristics at the FWHM of homogeneous broadenings (a) 10 meV (b) 15 meV, (c) 20 meV and (d) 30 meV and injection currents I = 2, 2.5, 5 and 10 mA for the FWHM of inhomogeneous broadening 20 meV

As shown in Fig. 7 modulation bandwidth and relaxation oscillation frequency increase as the injection current increases. This is due to the increase of carriers in central group of Qds.

Figure 8 also shows the modulation response at the injection currents (a) I = 8 and (b) I = 10 mA when the FWHM of homogeneous broadening is 0.1, 3, 5 and 10 meV. As the FWHM of homogeneous broadening increases, relaxation oscillation frequency and modulation bandwidth decrease. Modulation response amplitude until

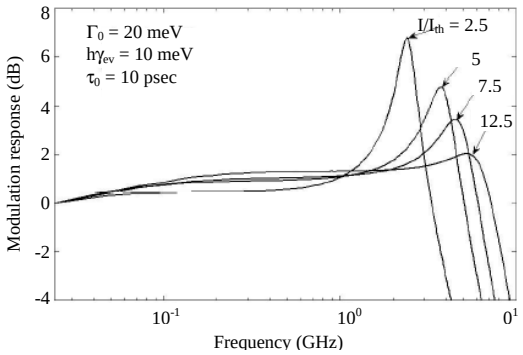

Fig. 7: Calculated modulation response of the RT lasing for different injection currents 2.5, 5, 7.5, 12.5

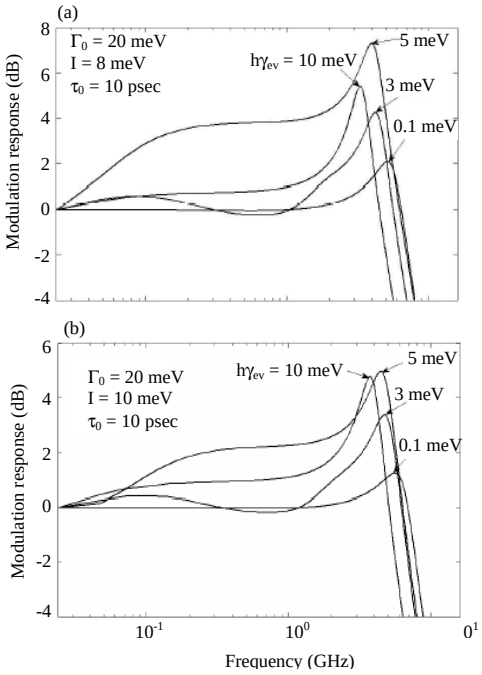

Fig. 8: Modulation response at (a) I = 5 mA and (b) I = 10 mA when the FWHM of homogeneous broadening is 0.1, 3, 5 and 10 meV

the FWHM of homogeneous broadening 10 meV decreases and then increases. Figure 9a shows the modulation response of the RT lasing for different FWHM of inhomogeneous broadenings 10, 20 and 40 meV. Relaxation oscillation frequency, modulation bandwidth, modulation response amplitude decrease as the FWHM of inhomogeneous broadening increases.

Figure 9b also shows the modulation response of the RT lasing for different initial carrier relaxation lifetimes 1, 10, 25, 50 and 100 psec.

Relaxation oscillation frequency, modulation bandwidth and modulation response amplitude decrease

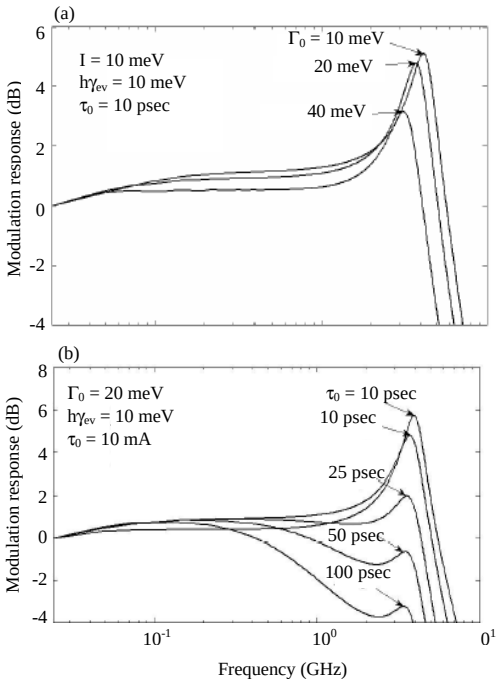

Fig. 9: Modulation response of the RT lasing for different (a) FWHM of inhomogeneous broadenings 10, 20 and 40 meV and (b) initial carrier relaxation lifetimes 1, 10, 25, 50 and 100 psec

as the carrier relaxation lifetime increases. Modulation response amplitude at the relaxation oscillation frequency for 100 psec reduces to -3.241 dB.

CONCLUSION

Self-assembled Quantum Dots (QDs) with broadband emitting spectra, QD Super Luminescent Diodes (SLDs) and external cavity tunable QD laser have been studied. The calculations show that the thermal carrier escape leads to shift the dominant lasing mode at the low injection currents. The number of lasing modes increases for the larger injection currents. With exceeding the FWHM of homogeneous broadening from the full width at half maximum FWHM of inhomogeneous broadening, the dynamic and static-characteristics degrade and SAQD-LD reaches the steady-state slower. The threshold current, the steady-state photons and the dynamic-characteristics degrade and SAQD-LD reaches the steady-state slower as the FWHM of inhomogeneous broadening and carrier relaxation life time increase.

ACKNOWLEDGMENT

The researchers would like to thank Maryam Gholvani for writing up the study.

REFERENCES

Bilenca, A. and G. Eisenstein, 2004. On the noise properties of linear and nonlinear quantum-dot semiconductor optical amplifiers: The impact of inhomogeneously broadened gain and fast carrier dynamics. IEEE J. Quantum Electron., 40: 690-702.

Grundmann, M., 2002. Nano-Optoelectronics: Concepts, Physics and Devices. 1st Edn., Springer-Verlag Berlin, pp: 442.

Liu, N., P. Jin and Z.G. Wang, 2005. InAs/GaAs quantum-dot super luminescent diodes with 110 nm bandwidth. Electron. Lett., 41: 1400-1402.

Lv, X.Q., N. Liu, P. Jin and Z.G. Wang, 2008. Broadband emitting super luminescent diodes with InAs quantum dots in AlGaAs matrix. IEEE Photon. Technol. Lett., 20: 1742-1744.

Markus, A., J.X. Chen, O. Gauthier-Lafaye, J.G. Provost, C. Paranthoen and A. Fiore, 2003. Impact of intraband relaxation on the performance of a quantum-dot laser. IEEE J. Sel. Top. Quantum Electron., 9: 1308-1314.

Sugawara, M., 1995. Theory of spontaneous-emission lifetime of Wannier excitons in mesoscopic semiconductor quantum disks. Phys. Rev. B Condens. Matter., 51: 10743-10754.

Sugawara, M., 1999. Self-Assembled InGaAs/GaAs Quantum Dots. Academic Press, New York, pp: 60.

Sugawara, M., K. Mukai, Y. Nakata and H. Ishikawa, 2000. Effect of homogeneous broadening of optical gain on lasing spectra in self-assembled InxGa1-xAs/GaAs quantum dot lasers. Phys. Rev. B, 61: 7595-7603.

Tan, C.L., Y. Wang, H.S. Djie and B.S. Ooi, 2007. Role of optical gain broadening in the broadband semiconductor quantum-dot laser. Applied Phys. Lett., 91: 061117-061119.

Tan, C.L., Y. Wang, H.S. Djie and B.S. Ooi, 2008. The role of optical gain broadening in the ultrabroadband InGaAs/GaAs interband quantum-dot laser. Comput. Mater. Sci., 44: 167-173.

Zhang, Z.Y., R.A. Hogg, P. Jin, T.L. Choi, B. Xu and Z.G. Wang, 2008. High-power quantum-dot superluminescent LED with broadband drive current insensitive emission spectra using tapered active region. IEEE Photon. Technol. Lett., 20: 782-784.